

# Effect of C/Ti Atom Ratio on the Deformation Behavior of $\text{TiC}_\chi$ Grown by FZ Method at High Temperature

Soon-Gi Shin<sup>†</sup>

Department of Advanced Materials Engineering, College of Samcheok, Kangwon National University, Samcheok, Gangwon-Do 245-711, Korea

(Received May 20, 2013 : Received in revised form July 16, 2013 : Accepted July 17, 2013)

**Abstract** In order to clarify the effect of C/Ti atom ratios( $\chi$ ) on the deformation behavior of  $\text{TiC}_\chi$  at high temperature, single crystals having a wide range of  $\chi$ , from 0.56 to 0.96, were deformed by compression test in a temperature range of 1183~2273 K and in a strain rate range of  $1.9 \times 10^{-4} \sim 5.9 \times 10^{-3} \text{ s}^{-1}$ . Before testing,  $\text{TiC}_\chi$  single crystals were grown by the FZ method in a He atmosphere of 0.3 MPa. The concentrations of combined carbon were determined by chemical analysis and the lattice parameters by the X-ray powder diffraction technique. It was found that the high temperature deformation behavior observed is the  $\chi$ -less dependent type, including the work softening phenomenon, the critical resolved shear stress, the transition temperature where the deformation mechanism changes, the stress exponent of strain rate and activation energy for deformation. The shape of stress-strain curves of  $\text{TiC}_{0.96}$ ,  $\text{TiC}_{0.85}$  and  $\text{TiC}_{0.56}$  is seen to be less dependent on  $\chi$ , the work hardening rate after the softening is slightly higher in  $\text{TiC}_{0.96}$  than in  $\text{TiC}_{0.85}$  and  $\text{TiC}_{0.56}$ . As  $\chi$  decreases the work softening becomes less evident and the transition temperature where the work softening disappears, shifts to a lower temperature. The  $\tau_c$  decreases monotonously with decreasing  $\chi$  in a range of  $\chi$  from 0.86 to 0.96. The transition temperature where the deformation mechanism changes shifts to a lower temperature as  $\chi$  decreases. The activation energy for deformation in the low temperature region also decreased monotonously as  $\chi$  decreased. The deformation in this temperature region is thought to be governed by the Peierls mechanism.

**Key words** titanium carbide, single crystal, deformation, high temperature, work softening.

## 1. Introduction

Titanium carbide, which will be hereafter described as  $\text{TiC}_\chi$  ( $\chi$  is C/Ti atom ratio), has the lowest density among the monocarbides of group IVa, Va transition metals, and exhibit electrical and thermal conductivities as good as those of metals. Hence it is expected to be used as additive of structure materials under severe environmental conditions. For such a practical use, as well as fundamental interests, it is important to clarify the mechanical properties of  $\text{TiC}_\chi$  at high temperatures. Another interesting characteristic of  $\text{TiC}_\chi$  is that  $\text{TiC}_\chi$  has nonstoichiometry over a wide range of  $\chi$  from about 0.5 to 1.0 without changing the crystal structure.<sup>1-4)</sup> Many investigations concerning the effect of  $\chi$  on deformation behavior of  $\text{TiC}_\chi$  at high temperature have been made so far. Samsonov<sup>5)</sup> reported that the Vickers hardness of sintered polycry-

stalline  $\text{TiC}_\chi$  with  $\chi$  from 0.73 to 0.94 decreases with decreasing  $\chi$  over the temperature range room temperature to 2270 K. Spivak<sup>6)</sup> carried out the high temperature creep test for hot-pressed polycrystalline  $\text{TiC}_\chi$ ,  $0.63 \leq \chi \leq 0.96$ , at very high temperature from 2370 to 2870 K and showed that the creep rate takes a minimum around  $\chi = 0.9$ . And Miracle<sup>7)</sup> conducted Vickers hardness, four point bending and compression tests for hot pressed polycrystalline  $\text{TiC}_\chi$  having  $\chi$  from 0.66 to 0.93 at temperature from room temperature to 1470 K and showed that the strength decreases with decreasing  $\chi$ .

In most of the above investigations, sintered or hot pressed polycrystalline samples were used. In these samples, and appreciable content of impurities is usually included and the impurities are liable to form second phases of low melting point at grain boundaries,<sup>8-10)</sup> thereby causing grain boundary sliding at relatively lower temperature

<sup>†</sup>Corresponding author

E-Mail : [ssg@kangwon.ac.kr](mailto:ssg@kangwon.ac.kr) (S. -G. Shin, Kangwon Nat'l Univ.)

© Materials Research Society of Korea, All rights reserved.

This is an Open-Access article distributed under the terms of the Creative Commons Attribution Non-Commercial License (<http://creativecommons.org/licenses/by-nc/3.0>) which permits unrestricted non-commercial use, distribution, and reproduction in any medium, provided the original work is properly cited.

which is different from the intrinsic mechanical properties of  $\text{TiC}_\chi$ .<sup>4-6)</sup> Further around pores stress concentration occurs depending on the size and shape of pores. In short, for sintered  $\text{TiC}_\chi$  the effects of impurities, grain boundaries and pores on the mechanical properties are significant. Therefore, for obtaining the reliable data on the effect of  $\chi$  on the mechanical properties of  $\text{TiC}_\chi$ , it is necessary to use well-characterized single crystals having no effect of grain boundaries and pores and negligible amounts of impurities. Such a single crystal experiment on the relation between high temperature deformation behavior of  $\text{TiC}_\chi$  and  $\chi$  was carried out only by Williams.<sup>11)</sup> However, the range of  $\chi$  was limited to relatively higher values ( $\chi \geq 0.79$ ), and his result was confined to the temperature dependence of critical resolved shear stress.

In the present research,  $\text{TiC}_\chi$  single crystals with a wide range of  $\chi$  from 0.56 to 0.96 were grown by the floating zone technique and deformed by the compression test at temperatures from 1183 to 2273 K and at strain rates from  $1.9 \times 10^{-4}$  to  $5.9 \times 10^{-3} \text{ s}^{-1}$  to investigate the effect of  $\chi$  on the shape of stress strain curves, the dependence of temperature and strain rate on the critical resolved shear stress.

## 2. Experimental Procedures

$\text{TiC}_{1.0}$  (average particle size 1.7  $\mu\text{m}$ , purity 99.8 %, Kojundo Chemical Co. Ltd.) and Ti powders (average particle size 2  $\mu\text{m}$ , purity 99.9 %, Mitsubishi Materials Co. Ltd.) were mixed so that the composition of  $\text{TiC}_\chi$  lay in a range from 0.56 to 0.96 in  $\chi$ , and then isostatically pressed at 200 MPa for 60 s into rods of 10 mm in diameter and 150 mm in length. The rods were degassed and presintered by r. f. induction heating at about 1550 K for 5.2 ks in a vacuum of 10 mPa and then fully sintered at 2670 K for 3.6 ks in a He atmosphere of 0.2 MPa. Single crystals were grown by the floating zone technique in a He atmosphere of 0.3 MPa. Specimens (size 2 mm  $\times$  2 mm  $\times$  3 mm) with single slip orientation were cut out from the single crystals with a low speed diamond cutter and then polished with emery papers and diamond paste. The concentrations of combined carbon were determined by chemical analysis and the lattice parameters by the X-ray powder diffraction technique. Table 1 shows the com-

**Table 1.** Chemical composition (mass %) and lattice parameter (nm) of  $\text{TiC}_\chi$ .

Composition	Carbon (total)	Lattice parameter
$\text{TiC}_{1.0}$	19.70	0.43273
$\text{TiC}_{0.96}$	19.31	0.43293
$\text{TiC}_{0.85}$	17.71	0.43303
$\text{TiC}_{0.56}$	12.84	0.43189

positions and lattice parameters  $\text{TiC}_{1.0}$ , and three kinds of single crystals.

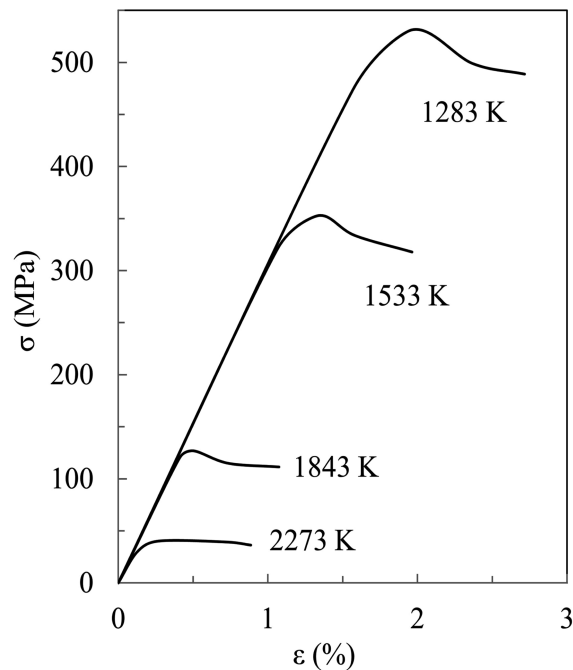
The compression test was conducted in a vacuum of 1.3 mPa at temperature from 1183 to 2273 K and at strain rates from  $1.9 \times 10^{-4}$  to  $5.9 \times 10^{-3} \text{ s}^{-1}$ . The details of the testing machine, heating method and temperature measurement used were the same as those described in previous papers.<sup>12,13)</sup>

## 3. Results

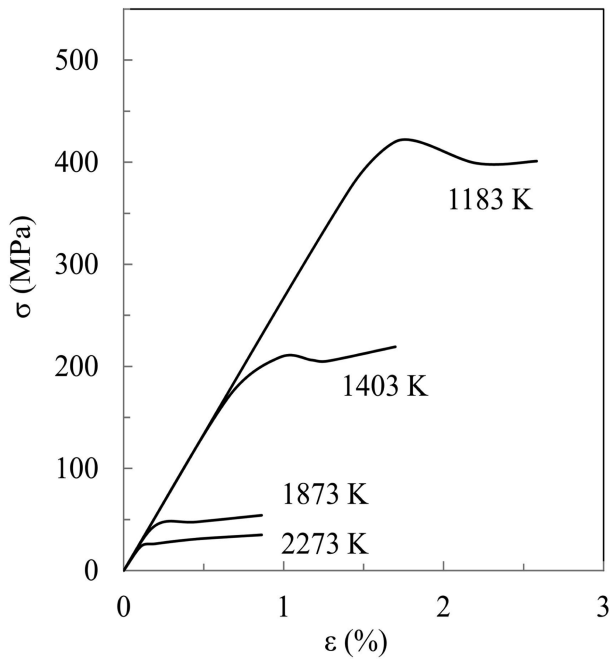
Figs. 1-3 show the temperature dependence of yielding behavior of  $\text{TiC}_{0.96}$ ,  $\text{TiC}_{0.85}$  and  $\text{TiC}_{0.56}$  compressed at a strain rate of  $5.9 \times 10^{-4} \text{ s}^{-1}$ . At lower temperatures the work softening phenomenon occurs irrespectively of composition, however, it tends to become less evident with decreasing  $\chi$ .

Fig. 4 shows general shapes of stress-strain curves of  $\text{TiC}_{0.96}$ ,  $\text{TiC}_{0.85}$  and  $\text{TiC}_{0.56}$  compressed at 1283 K and at a strain rate of  $1.9 \times 10^{-3} \text{ s}^{-1}$ . The shape is seen to be less dependent on  $\chi$ , the work hardening rate after the softening is slightly higher in  $\text{TiC}_{0.96}$  than in  $\text{TiC}_{0.85}$  and  $\text{TiC}_{0.56}$ .

Fig. 5 shows the temperature dependence of critical resolved shear stress ( $\tau_c$ ), which corresponds to the upper yield stress when the work softening is present and to the 0.2 % proof stress when it is absent. The value of  $\tau_c$  decreases monotonously with increasing temperature.  $\tau_c$  is normalized by the shear modulus ( $G$ ),<sup>2,14)</sup> and plotted against the reciprocal of temperature in Fig. 6. The



**Fig. 1.** Temperature dependence of yield behavior for  $\text{TiC}_{0.96}$  compressed at a strain rate of  $5.9 \times 10^{-4} \text{ s}^{-1}$ .



**Fig. 2.** Temperature dependence of yield behavior for  $TiC_{0.85}$  compressed at a strain rate of  $5.9 \times 10^{-4} s^{-1}$ .

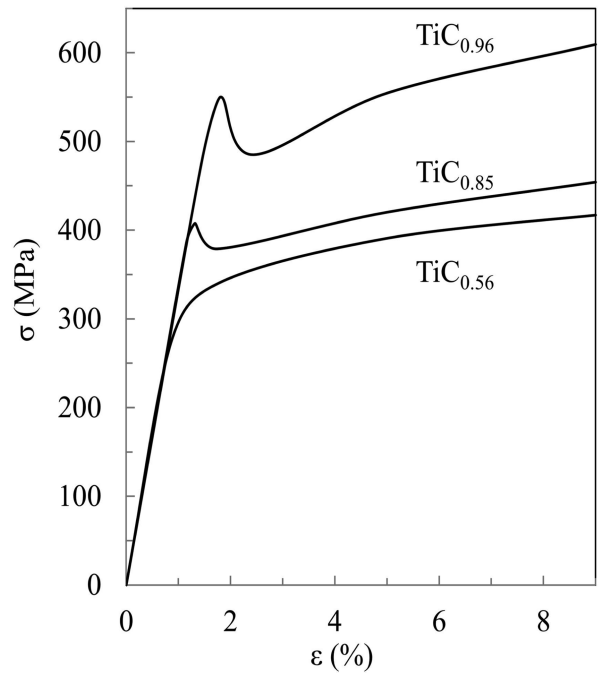


**Fig. 4.** Stress-strain for  $TiC_{0.96}$ ,  $TiC_{0.85}$  and  $TiC_{0.56}$  compressed at 1283 K at a strain rate of  $1.9 \times 10^{-4} s^{-1}$ .

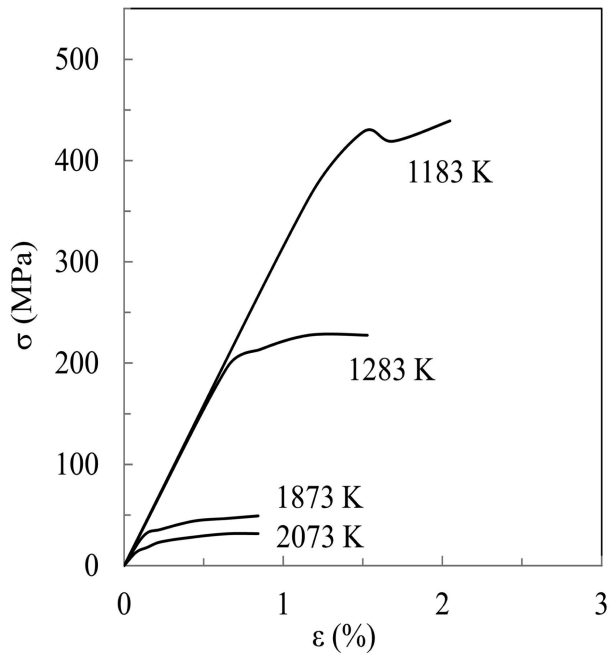


**Fig. 3.** Temperature dependence of yield behavior for  $TiC_{0.56}$  compressed at a strain rate of  $5.9 \times 10^{-4} s^{-1}$ .

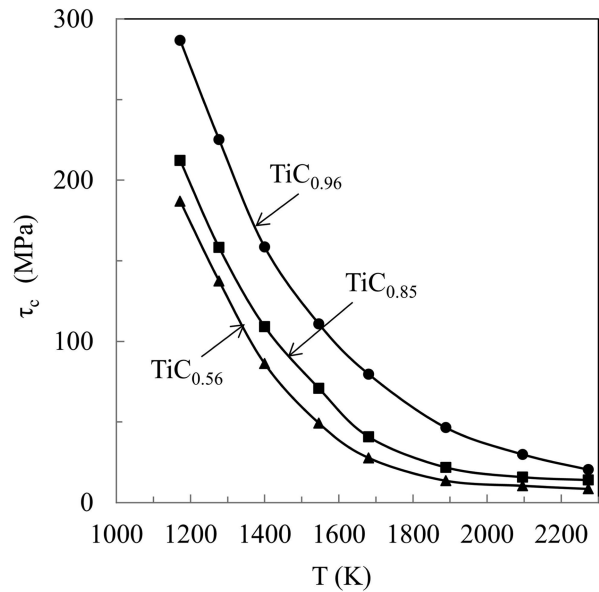


**Fig. 5.** Temperature dependence of critical resolved shear stress( $\tau_c$ ) for  $TiC_{0.96}$ ,  $TiC_{0.85}$  and  $TiC_{0.56}$  compressed at a strain rate of  $5.9 \times 10^{-4} s^{-1}$ .

curves are divided into two parts with different slopes by a transition temperature( $T_c$ ); the low and high temperature regions. It is also seen that the value of  $T_c$  is the highest for  $TiC_{0.96}$  and decreases in the following order;  $TiC_{0.96} \rightarrow TiC_{0.85} \rightarrow T_{0.56}$ ;  $T_c$  decreases with decreasing  $\chi$ .

Figs. 7, 8 show the double-logarithmic plot of  $\tau_c/G$  against plastic shear strain rate( $\dot{\gamma}$ ). It is seen that there is

a good linear relationship between  $\log(\tau_c/G)$  and  $\log \dot{\gamma}$ . The reciprocal of the slope of these straight lines gives the stress exponent of the strain rate( $m$ ).<sup>12,14</sup> Since our previous research<sup>12,13</sup> showed that in each of the two temperature regions the value of  $m$  is less dependent on temperature, in the present work  $m$  was measured at two temperatures of 1283(Fig. 7) and 2083 K(Fig. 8). The

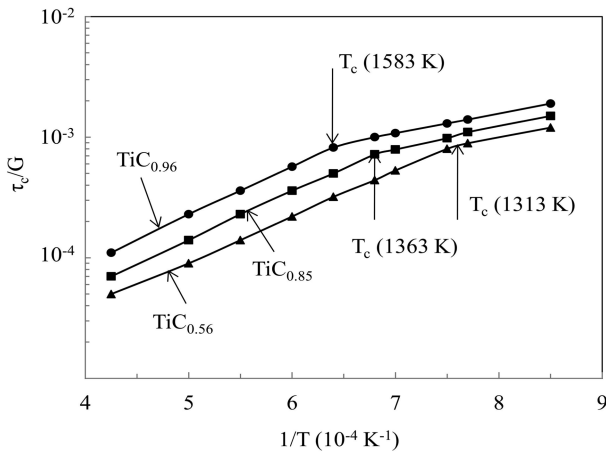


**Fig. 6.**  $\text{Log}(\tau_c/G)$  vs.  $1/T$  for  $\text{TiC}_{0.96}$ ,  $\text{TiC}_{0.85}$  and  $\text{TiC}_{0.56}$  compressed at a strain rate of  $5.9 \times 10^{-4} \text{ s}^{-1}$ . The arrows indicate the transition temperature of mechanism controlling deformation ( $T_c$ ).

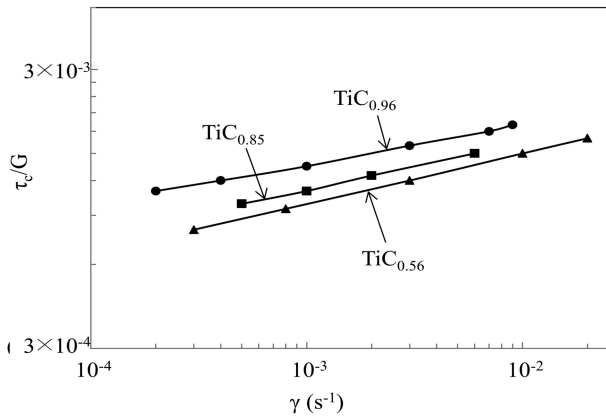


**Fig. 7.**  $\text{Log}(\tau_c/G)$  vs.  $\text{log } \gamma$  at 1283 K for  $\text{TiC}_{0.96}$ ,  $\text{TiC}_{0.85}$  and  $\text{TiC}_{0.56}$ .

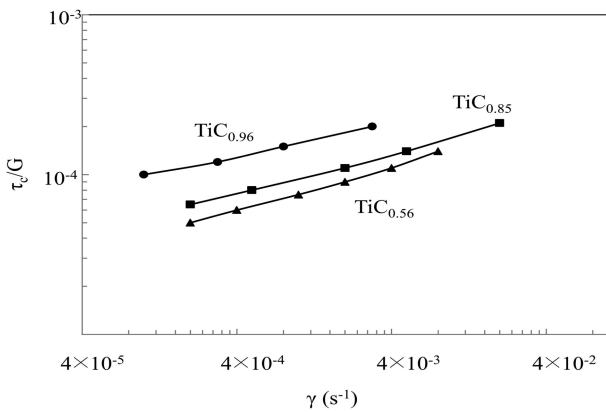


**Fig. 8.**  $\text{Log}(\tau_c/G)$  vs.  $\text{log } \gamma$  at 2083 K for  $\text{TiC}_{0.96}$ ,  $\text{TiC}_{0.85}$  and  $\text{TiC}_{0.56}$ .

result is shown in Table 2. In the high temperature region,  $m$  does not depend significantly on  $\chi$ ;  $m = 4.93$ . In the low temperature region, however,  $m$  is dependent on  $\chi$ ;  $m = 10$  in higher  $\chi (= 0.96)$  and  $m = 6$  in lower  $\chi (= 0.56)$ .

Fig. 9 is a plot of  $\tau_c$  at the upper yield points against  $\chi$ .

**Table 2.** Values of  $m$  and  $Q$  in the high and low temperature regions.

	High temperature region		Low temperature region	
	$m$	$Q(\text{kJ/mol})$	$m$	$Q(\text{kJ/mol})$
$\text{TiC}_{0.96}$	5.3	470	10	300
$\text{TiC}_{0.85}$	4.8	359	9	259
$\text{TiC}_{0.56}$	4.7	318	6	179

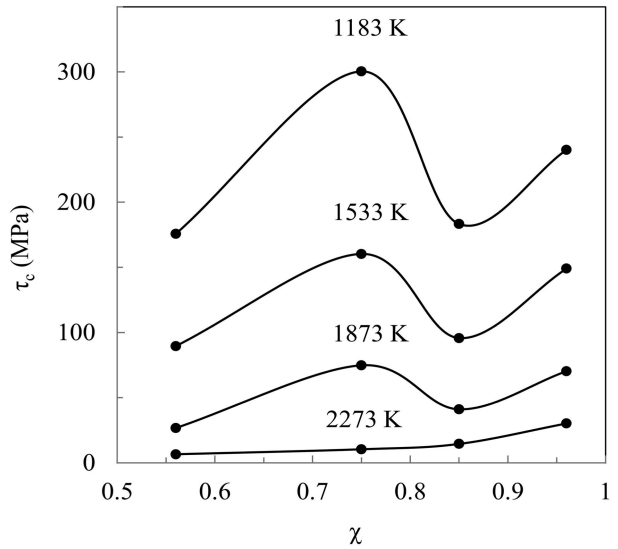


**Fig. 9.** Dependence of  $\tau_c$  on C/Ti atom ratio ( $\chi$ ) for  $\text{TiC}_\chi$  compressed at a strain rate of  $5.9 \times 10^{-4} \text{ s}^{-1}$ .  $\tau_c$  is the values at upper yield point.

It is noted that  $\chi$  dependence of  $\tau_c$  varies with temperature and the dependence is very marked at lower temperatures. In the lower temperature region,  $\tau_c$  decreases monotonously with decreasing  $\chi$  in a range of  $\chi = 0.96$  to  $0.85$ , in agreement with the result of Williams,<sup>11)</sup> but increases with further decrease in  $\chi$  and  $\tau_c$  takes a peak  $\chi = 0.75$ . The value of  $\tau_c$  decreases again at  $\chi = 0.56$ . The peak in  $\tau_c$  at  $\chi = 0.75$  lowers with increasing temperature and finally disappears at 2273 K.

From the result described in Figs. 5-8, the relation between the plastic shear strain rate ( $\dot{\gamma}$ ), the critical resolved shear stress ( $\tau_c$ ) and the absolute temperature ( $T$ ), is expressed as  $\dot{\gamma} = A(\tau_c/G)^m \exp(-Q/RT)$ , where  $A$  is constant,  $Q$  the activation energy for deformation and  $R$  the gas constant.  $Q$  obtained from the slope of Fig. 6, which gives  $Q/Rm$ , and the stress exponent ( $m$ ), for the high and low temperature regions are listed in Table 2. The value of  $Q$  depends on  $\chi$  and decreases with decreasing  $\chi$  in each of the two temperature regions.

#### 4. Discussion

The results obtained in the present research show that the high temperature deformation behavior of  $\text{TiC}_\chi$  is the

$\chi$  less-dependent type<sup>12)</sup> includes work softening phenomenon, the critical resolved shear stress, the transition temperature where the deformation mechanism changes, the stress exponent of strain rate, in the low temperature region and the activation energy for the deformation in the low and high temperature regions. Each of these behaviors will be discussed below.

The work softening phenomenon became less clear with decreasing  $\chi$ . For the decrease in  $\chi$ , two effects should be considered: one is the effect of increasing the interaction between dislocations and carbon vacancies, and the other is the effect of decreasing the Peierls barrier.<sup>5,12)</sup> The elastic interaction between dislocations and vacancies is short range and will decrease with an increase in dislocation density due to deformation. Therefore, if the increasing effect of dislocation-vacancy interaction is dominant, the work softening, which is caused by the decrease in the mean dislocation velocity, should become more conspicuous with decreasing  $\chi$ . On the contrary, if the decreasing effect of the Peierls stress<sup>15)</sup> due to a decrease in  $\chi$  is dominant, the effective stress acting for dislocation motion decreases and the work softening should become less evident as  $\chi$  decreases. Therefore, the present result that the work softening decreased with decreasing  $\chi$  supports the view that the decreasing effect of the Peierls stress is dominant compared with the increasing effect of dislocation-vacancy interaction.

It was found in this research that  $\tau_c$  does not decrease monotonously with decreasing  $\chi$  and the  $\chi$ -dependence of  $\tau_c$  varies with temperature. The  $\chi$  dependence of  $\tau_c$  was similar to that of work softening and may be understood in the manner as the case of work softening. Williams<sup>11)</sup> showed that there is a good linear relationship between  $\tau_c$  and  $\chi$  in a range of  $\chi$  from 0.79 to 0.95 over the temperature range 1080 to 1870 K. Also in the present research, similar results were obtained in almost the same composition range (Fig. 9); however, the slope of the linear part was much steeper and absolute value of  $\tau_c$  was higher by approximately 20% than those in the result of Williams. These differences may come from the differences in the degree of perfection of crystals, the composition direction and the rigidity of machine used.<sup>13)</sup>

There are some reports which described the transition temperature ( $T_c$ ) similar to Fig. 6. However, the values of  $T_c$  reported so far are considerably different from each other. This difference may come from the differences in carbon/titanium atom ratio, the impurity content, the degree of perfection such as the initial dislocation density.<sup>13)</sup> Yoshinaga<sup>16)</sup> showed that  $T_c$  shifts to higher temperatures as the strain rate increases. As seen from the  $\gamma = \rho_m b v$  and  $v = B \tau_e^{m^*} \propto \exp(-Q/RT) \tau_e^{m^*}$ ,<sup>12,13,15)</sup> where  $\rho_m$  is the mobile dislocation density,  $b$  the magnitude of Burgers vector,  $B$  the mobility of dislocations,  $m^*$  the effective

stress exponent of dislocation velocity,  $\tau_e^{m^*}$  effective stress, the increase in  $\gamma$  may result mainly from the increase in dislocation velocity ( $v$ ). Furthermore, the decrease in flow stress above  $T_c$  was shown to be caused by the diffusion of carbon atoms which act as the barrier to dislocation motion (carbon diffusion mechanism).<sup>14,15)</sup> Therefore,  $T_c$  is considered to depend on the relative magnitude of  $v$  to carbon diffusion rate: when  $v$  becomes faster, the decrease in flow stress is not expected to occur until the carbon atoms can diffuse along with dislocations, which may result in the shift of  $T_c$  to higher temperatures with increasing strain rate. In this research, the effect of variation in impurity content with  $\chi$  is assumed to be negligible and the other parameters are almost the same, and thus we can discuss the effect of nonstoichiometry on  $T_c$  of TiC<sub>χ</sub>. For the carbon diffusion controlling deformation, the value of  $Q$  in  $v = B \tau_e^{m^*} \propto \exp(-Q/RT) \tau_e^{m^*}$  may correspond to the activation energy for carbon self-diffusion ( $Q_d^c$ ). Provided that in the strain rate constant test the initial dislocation density in samples used is the same and the value of  $d\rho_m/d\varepsilon$  is independent of composition, the temperature at which carbon atoms can diffuse along with dislocations moving at a velocity  $v$  should decrease as the value of  $Q_d^c$  decreases. Since the activation energy for deformation in the high temperature region was found to decrease with decreasing  $\chi$  (Table 2), one can understand that  $T_c$  shifts to lower temperatures as  $\chi$  decreases.

It is well known that stress exponent ( $m$ ) of strain rate, is related to the effective stress exponent ( $m^*$ ) of  $v$ , by  $m = m^*/(1 - \tau_i/\tau)$ . In this research, the value of  $m$  obtained in the low temperature region decreased with decreasing  $\chi$ . This can be attributed to a decrease in  $m^*$  or  $\tau_i/\tau$  or both with decreasing  $\chi$ , as seen from  $m = m^*/(1 - \tau_i/\tau)$ . As shown in detail in previous paper<sup>12,13)</sup> and Kurishita,<sup>17)</sup> the dislocations distribute inhomogeneously in high  $\chi$  samples ( $0.86 \leq \chi \leq 0.95$ ), whereas in low  $\chi$  samples ( $\chi = 0.59$  and  $0.75$ ), their distribution is fairly uniform and many junctions are formed. The junction formation is thought to indicate a significant contribution of the secondary slip system to deformation. The fairly homogeneous distribution and the activation of the secondary slip system suggest that the value of  $m^*$  is small.<sup>18-21)</sup> On the other hand, if  $m^*$  is small, marked work softening is expected to occur. However, in TiC<sub>0.56</sub> the work softening became less marked in spite of the smallest value of  $m$ . This disagreement suggests that the magnitude of work softening cannot be definitely correlated to the value of  $m^*$ .

Since the deformation in the high temperature region is considered to be controlled by carbon diffusion as mentioned previously, the observed decrease in the activation energy for deformation with decreasing  $\chi$  suggests that the height of potential barrier on the diffusion path of carbon

atoms depends on composition. On the other hand, the activation energy for deformation in the low temperature region also decreased monotonously as  $\chi$  decreased. Since the deformation in this temperature region is thought to be governed by the Peierls mechanism,<sup>14,15,22</sup> it appears that the observed decrease in activation energy with decreasing  $\chi$  is correlated to a decrease in the Peierls barrier due to the decreasing in titanium-carbon bond strength as  $\chi$  decreases.

#### 4. Conclusions

In order to clarify the effect of C/Ti atom ratio( $\chi$ ) on the high temperature deformation behavior of  $\text{TiC}_\chi$ , crystals in a wide range of  $\chi$  from 0.56 to 0.96 were grown by FZ method and subjected to the high temperature compression test at temperatures from 1183 to 2273 K and at strain rates from  $1.9 \times 10^{-4}$  to  $5.9 \times 10^{-3}$ /s. The high temperature deformation behavior of  $\text{TiC}_\chi$  is the  $\chi$  less-dependent type includes work softening phenomenon, the critical resolved shear stress, the transition temperature where the deformation mechanism changes, the stress exponent of strain rate, in the low temperature region and the activation energy for the deformation in the low and high temperature regions. As  $\chi$  decreases the work softening becomes less evident and transition temperature where the work softening disappear shifts to a lower temperature. The  $\tau_c$  decreases monotonously with decreasing  $\chi$  in a range of  $\chi$  from 0.86 to 0.96. The transition temperature where the deformation mechanism changes shifts to a lower temperature as  $\chi$  decreases.

#### References

1. E. K. Storms, *The Refractory Carbides*, Academic Press, New York (1967).
2. I. Miyake and T. Tanase, *Cemented Carbide and Sintered Hard Materials (Basic and Application)* (ed. H. Suzuki), p.307, Maruzen, Tokyo (1986).
3. S. G. Shin, Ph.D. Thesis (in Japanese), p.83-94, University of Tokyo, Tokyo (1992).
4. S. G. Shin, *Kor. J. Met. Mater.*, **48**(9), 825 (2010).
5. G. V. Samsonov, M. S. Kovalchenko, V. V. Dzemelinskii and D. S. Upadyaya, *Phys. Status Solid (a)*, **1**, 327 (1970).
6. I. I. Spivak, R. A. Andrievskii, V. N. Rystsov and V. V. Klimenko, *Poroshkovata Met.*, **139**, 69 (1974).
7. D. B. Miracle and H. A. Lipsitt, *J. Amer. Ceram. Soc.*, **66**, 592 (1983).
8. A. P. Katz, H. A. Lipsitt, T. Mah and M. G. Mendiratta, *J. Mater. Sci.*, **18**, 1983 (1983).
9. G. Das, K. S. Mazdiyasi and H. A. Lipsitt, *J. Amer. Ceram. Soc.*, **65**, 104 (1982).
10. V. M. Sura and D. L. Kohlstedt, *J. Mater. Sci.*, **21**, 2356 (1986).
11. W. S. Williams, *J. Appl.*, **35**, 1329 (1964).
12. S. G. Shin, *Korean J. Met. Mater.*, **51**(7), 515 (2013).
13. S. G. Shin, to be published (in *Korean J. Met. Mater.*)
14. H. Kurishita, K. Nakajima and H. Yoshinaga, *Mater. Sci. Eng.*, **54**, 177 (1982).
15. T. Ohji, *Frontiers of Next-Generation Structural Materials-Impact on Society and Industry-* (ed. N. Shinya), p.161, cmcbooks, Tokyo (2008).
16. H. Yoshinaga and H. Kurishita, *Transition Metal Carbides and Their Composites*, in *Creep behavior of Crystalline Solids* (ed. By B. Wilshire and R. W. Evans), p.311, Pineridge Press (1985).
17. H. Kurishita, H. Yoshinaga, F. Takao and S. Goto, *J. Jpn. Inst. Met (in Japanese)*, **44**(4), 395 (1980).
18. H. Yoshinaga, *Bull. Japan Inst. Metals (in Japanese)*, **17**, 414 (1978).
19. G. H. Zhang, Y. U. Heo, E. J. Song and D. W. Suh, *Met. Mater. Int.* **19**(2), 153 (2013).
20. S. H. Byun, N. H. Kang, T. H. Lee, S. K. Ahn, H. W. Lee, *Met. Mater. Int.*, **18**(2), 201 (2012).
21. P. L. Gong and H. Li, *Electron. Mater. Lett*, **8**(2), 471 (2012).
22. S. C. Ur, E. S. Kim and S. H. Yi, *Electron. Mater. Lett*, **9**(2), 119 (2013).